Chemical Science

ROYAL SOCIETY OF CHEMISTRY

EDGE ARTICLE

View Article Online
View Journal | View Issue

Cite this: *Chem. Sci.*, 2020, **11**, 6539

All publication charges for this article have been paid for by the Royal Society of Chemistry

Testing the limits of radical-anionic CH-amination: a 10-million-fold decrease in basicity opens a new path to hydroxyisoindolines *via* a mixed C–N/C–O-forming cascade†

Quintin Elliott, Gabriel dos Passos Gomes, ‡ Christopher J. Evoniuk and Igor V. Alabugin *

An intramolecular C(sp^3)–H amidation proceeds in the presence of *t*-BuOK, molecular oxygen, and DMF. This transformation is initiated by the deprotonation of an acidic N–H bond and selective radical activation of a benzylic C–H bond towards hydrogen atom transfer (HAT). Cyclization of this radical–anion intermediate en route to a two-centered/three-electron (2c,3e) C–N bond removes electron density from nitrogen. As this electronegative element resists such an "oxidation", making nitrogen more electron rich is key to overcoming this problem. This work dramatically expands the range of N-anions that can participate in this process by using amides instead of anilines. The resulting 10^7-fold decrease in the N-component basicity (and nucleophilicity) doubles the activation barrier for C–N bond formation and makes this process nearly thermoneutral. Remarkably, this reaction also converts a weak reductant into a much stronger reductant. Such "reductant upconversion" allows mild oxidants like molecular oxygen to complete the first part of the cascade. In contrast, the second stage of NH/CH activation forms a highly stabilized radical–anion intermediate incapable of undergoing electron transfer to oxygen. Because the oxidation is unfavored, an alternative reaction path opens *via* coupling between the radical anion intermediate and either superoxide or hydroperoxide radical. The hydroperoxide intermediate transforms into the final hydroxyisoindoline products under basic conditions. The use of TEMPO as an additive was found to activate less reactive amides. The combination of experimental and computational data outlines a conceptually new mechanism for conversion of unprotected amides into hydroxyisoindolines proceeding as a sequence of C–H amidation and C–H oxidation.

Received 23rd December 2019
Accepted 14th February 2020

DOI: 10.1039/c9sc06511c

rsc.li/chemical-science

Introduction

Due to their abundance, C(sp^3)–H bonds offer an excellent starting point for the functionalization of organic compounds.[1] However, the productive use of C–H bonds is complicated due to the difficulties associated with their selective activation.[2] These challenges prompt chemists to search for new approaches for utilizing C–H bonds as a reactive organic functionality.[3]

C–H amination couples C–H activation with the concomitant formation of a C–N bond and opens new avenues for the synthesis of nitrogen-containing organic compounds.[4] This approach has evolved into a versatile group of reactions that overcome the challenges with C–H activation and C–N bond formation. Depending upon nitrogen's participation in C–H activation and C–N bond formation, one can broadly classify C–H amination reactions within the following four approaches: (a) C–H activation directly coupled with C–N bond formation (direct activation), (b) C–H activation with delayed C–N bond formation, (c) N-assisted C–H activation, and (d) independent C–H/N–H activation (Scheme 1).

In direct activation (Scheme 1a), nitrogen is responsible for the activation of C–H bonds and the formation of both the C–N and the N–H bonds. This mode of activation works with highly coordinatively unsaturated species, *e.g.*, nitrenes and nitrenium ions, where nitrogen can insert into a C–H bond in either a stepwise or concerted manner.[5]

In C–H activation with delayed C–N bond formation (Scheme 1b), nitrogen assists in C–H activation by breaking the C–H bond, but the C–N bond forming step needs an *additional* participant (*e.g.*, an external oxidant). This process also requires an electron-deficient nitrogen-centered intermediate, *i.e.*,

Department of Chemistry and Biochemistry, Florida State University, Tallahassee, Florida 32306, USA. E-mail: alabugin@chem.fsu.edu

† Electronic supplementary information (ESI) available: Experimental details, compound characterization, and computational details for all calculated structures. CCDC 1973775. For ESI and crystallographic data in CIF or other electronic format see DOI: 10.1039/c9sc06511c

‡ Current address: Department of Chemistry and Department of Computer Science, University of Toronto, Toronto, Ontario, Canada.

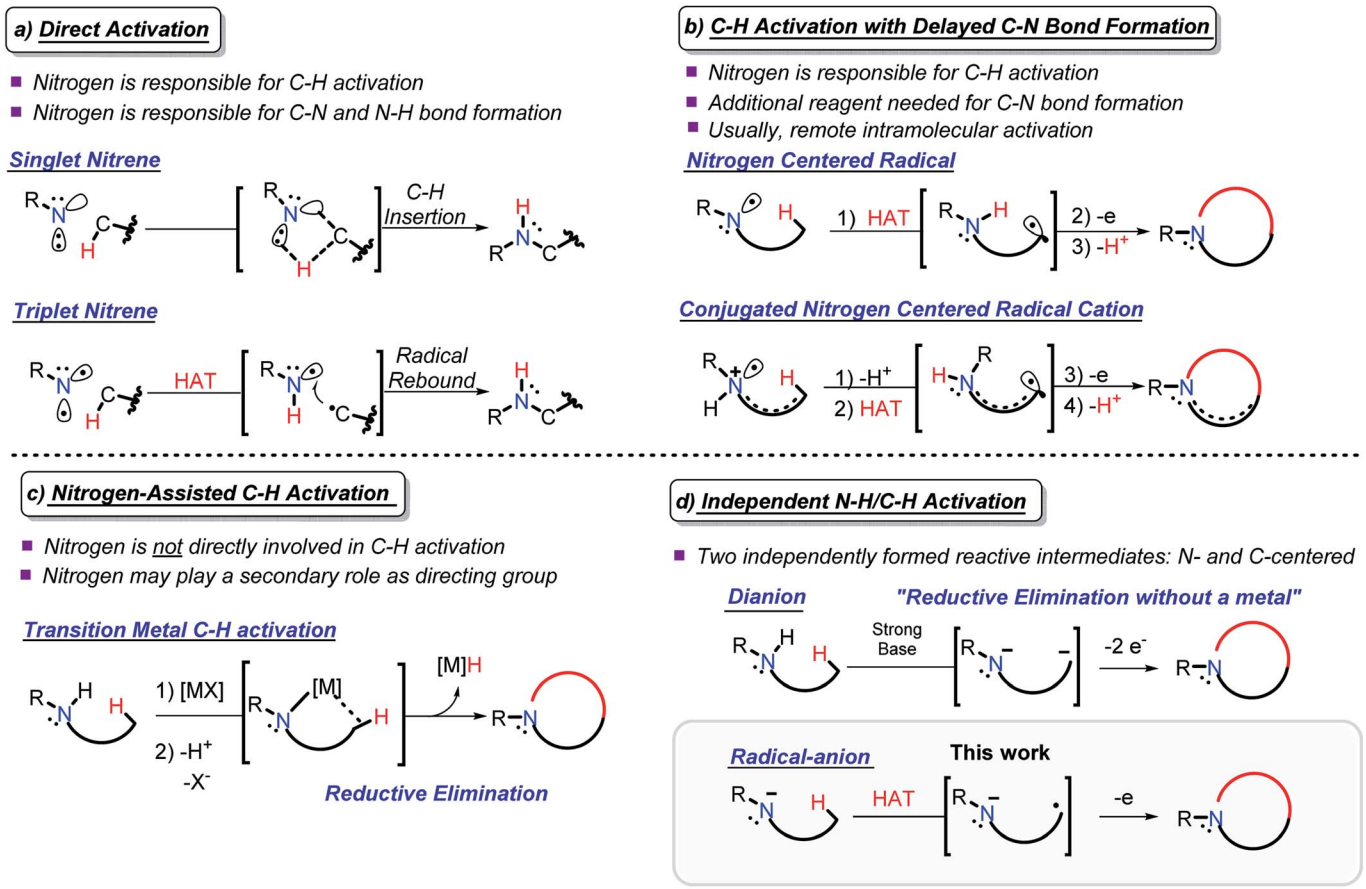

Scheme 1 Selected examples of the four approaches to C–N bond formation *via* C–H activation. All carbons are tetravalent, the non-participating C–H bonds are omitted for clarity.

a radical[6] or a radical–cation.[7] If placed in proximity to a C–H bond, a nitrogen-centered radical can abstract a hydrogen atom, forming a carbon centered radical. A C–N bond is formed by trapping this radical. Alternatively, activation of a C–H bond can be achieved by deprotonation of a nitrogen radical–cation, prepared by oxidation of an amine. Although such deprotonation usually proceeds at the α-position where it can provide a stabilized C-centered α-radical,[8] activation of a remote C–H bond becomes possible in conjugated radical–cations, even when the activating NH_2 moiety and the activated CH_2 group are five bonds away.[9,10]

In N-*assisted* C–H activation reactions (Scheme 1c), nitrogen does not *directly* participate in the C–H activation step but can trap the C-centered reactive species once they are formed. An external reagent, such as an appropriately chosen transition metal, is used for C–H activation. An appealing strategy is to use nitrogen as a directing group, guiding the transition metal to the targeted C–H bond and facilitating C–N bond formation afterwards.[11,12] A new C–N bond can be formed *via* reductive elimination at the transition metal.[13]

The fourth, conceptually different approach is to activate *both* the N–H and the C–H bonds by independently converting them into reactive intermediates (Scheme 1d). By decoupling the two steps, this approach potentially becomes the most flexible, but the conditions for selective and independent N–H/C–H activation are not always easy to achieve. The possible situations here involve: (i) formation of N- and C-centered radicals, (ii) formation of a radical and an anion (usually, C-radical and N-anion), and (iii) formation of an N-anion and a C-anion. The latter two paths must be terminated by 1e and 2e oxidations, respectively, to yield the "normal" two-centered/two-electron (2c,2e) C–N bond.

Productive combination of two reactive intermediates is efficient only when one of these intermediates is relatively persistent.[14] From this perspective, formation of stable N-anions (approaches ii and iii) is attractive (Scheme 1d).

Sarpong and coworkers illustrated that a C, N dianion, formed in the presence of strong base can form a C–N bond upon two-electron oxidation with I_2 (iii).[15] This approach, which can be conceptually considered "reductive elimination without a metal", allows C–N bond formation without the need for preoxidized coupling partners *via* the formal loss of H_2. Formation of five-, six-, and seven-membered rings was found to proceed even in conformationally unbiased substrates.

In our work, we explore the advantage of a three-electron approach (ii).[10] Because the three electron radical/anion

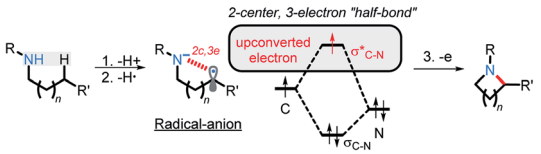

Scheme 2 Steps in the proposed C–H/N–H activation and the mechanism of electron upconversion.

interactions are potentially stabilizing, they can lead to favorable C/N precoordination which leads to instantaneous C–N bond formation upon oxidation. In contrast, the 4e anion/anion interactions are repulsive, and hence, the C,N-dianion may adopt a conformation that is not conducive to bond formation.

We have recently illustrated the value of the radical-anionic approach in an intramolecular C(sp^3)–H amination.[10] This method relies on a sequence of N–H deprotonations and selective H-atom transfers (HAT) from C–H bonds to generate a radical–anion intermediate (Scheme 3a). This intermediate forms a thermodynamically favored two-center/three-electron (2c,3e) "half bond", where one of the electrons is forced to occupy a high energy antibonding orbital ("electron upconversion", Scheme 2).[16] The newly formed radical–anion can then be readily oxidized into a "normal" 2c,2e bond by a mild oxidant, such as molecular oxygen. By generating a radical anion *in situ*, we effectively take a weak reductant and evolve it into a more potent reductant. Such "electron upconversion"[16] allows for the effective use of a mild oxidant such as molecular oxygen. By avoiding stronger oxidants, we prevented undesired product oxidation in our cascade reactions that yield expanded N-doped polyaromatic systems.

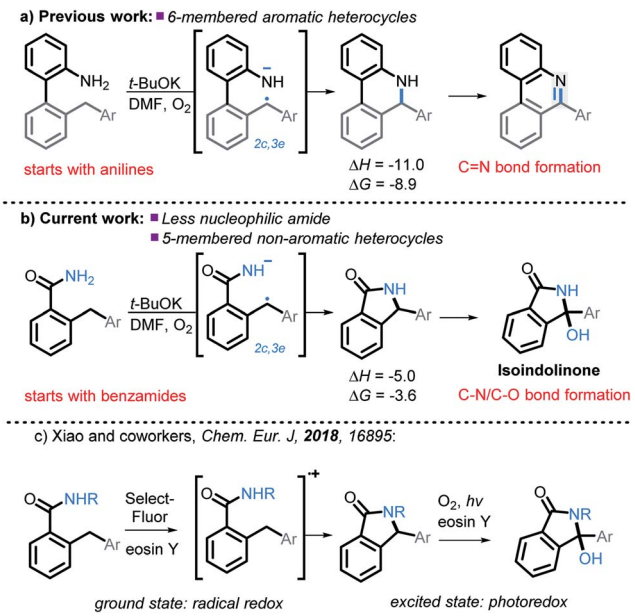

Scheme 3 Expanding previous work to utilize less nucleophilic amides, as well as the formation of non-aromatic five membered heterocycles, and C–N/C–O bond formation. All energies are in kcal mol^{-1}.

In this manuscript, we push the limits of this approach by using amides, a drastically less nucleophilic nitrogen source (Scheme 3b). We will show how this structural modification diverts the cascade towards incorporation of a late C–O bond forming step[17] and opens a synthetic route to 3-hydroxyisoindolinones. Recently, Xiao *et al.*[18] independently developed a mechanistically different version of 3-hydroxyisoindolinone synthesis from secondary amides (Scheme 3c). An interesting feature of Xiao's work is that the same catalyst is used in two different ways to promote the two cascade stages. In the first ground state stage, eosin Y acts as a radical redox catalyst which is oxidized to a radical–cation by reaction with a stoichiometric amount of an external oxidant (SelectFluor). Without light, the reaction stops at the first step (C–N bond formation). The second step (the formation of the C–O bond) is achieved by using eosin Y as a photocatalyst in the presence of oxygen. The overall transformation had a good scope for the aromatic substituents but was only reported for *N*-monosubstituted amides (*N*-methoxy, *N*-aryl, *N*-alkyl).

It is clear that our approach and the approach of Xiao are very different mechanistically (anionic *vs.* cationic) and, hence, should provide complementary reactivity patterns for future synthetic designs. Our work presents an alternative route that proceeds in the ground state and does not require additional oxidants besides molecular oxygen. In addition, it avoids formation of a cationic species, a feature which can be beneficial to substrates that are sensitive to oxidative conditions. Furthermore, as we will show below, our conditions are applicable for primary amides.

The successful use of amides as nucleophilic partners in a base-promoted oxidative C(sp^3)–H amidation yields isoindolinones under transition-metal free conditions. Because the presence of metal impurities should be minimized in pharmaceutics,[19] a transition-metal free alternative is an attractive choice for the synthesis of isoindolinones related to the antihypertensive agent chlortalidone,[20] inhibitors of MDM2-p53 interactions,[21] and selected natural products.[22] Furthermore, a variety of post-synthetic modifications of the core hydroxyisoindoline structure are possible (Scheme S5 in ESI†) including transformations mediated by chiral phosphoric acids[23,24] and by transition metal catalysts.[25]

Results and discussion

We began by subjecting amide **1a** (0.01 mmol) to the previously optimized conditions, (*i.e.*, DMF, 4 Å-molecular sieves (MS), O_2 atmosphere, and 3 equivalents of *t*-BuOK at room temperature) for 4 hours.[9] To our delight, **2a** was formed in an excellent yield, 87% (Table 1, entry 1). When DMSO and THF were used in place of DMF, the yields of **2a** were lower (36% and 47%, entries 2 and 5) along with the formation of undesired side products. Furthermore, when DMF was replaced with acetonitrile, toluene, or DCM, **2a** was not observed (entry 3, 4 and 6). These results prompted us to perform the rest of our studies in DMF.

We then tested five additional bases (entry 7–11). The *tert*-butoxide salts produced **2a** in the highest yields. Interestingly, the size of the counterion impacts the conversion of **1a** into **2a**.

Table 1 Optimization table[a]

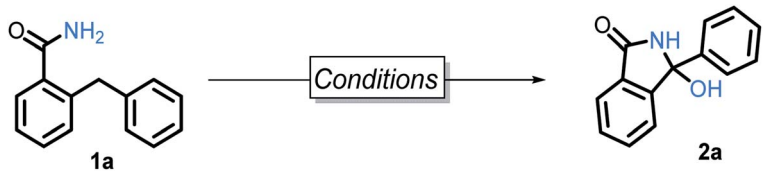

Entry	Solvent	Base	Eq.	Atm	Time	Yield%
1	DMF	*t*-BuOK	3	O_2	4 h	87%
2	DMSO	*t*-BuOK	3	O_2	4 h	36%
3	MeCN	*t*-BuOK	3	O_2	4 h	<1%
4	Toluene	*t*-BuOK	3	O_2	4 h	<1%
5	THF	*t*-BuOK	3	O_2	4 h	47%
6	DCM	*t*-BuOK	3	O_2	4 h	<1%
7	DMF	*t*-BuONa	3	O_2	4 h	79%
8	DMF	KOH	3	O_2	4 h	55%
9	DMF	NaOH	3	O_2	4 h	31%
10	DMF	LiOH	3	O_2	4 h	<1%
11	DMF	K_2CO_3	3	O_2	4 h	<1%
12	DMF	*t*-BuOK	1	O_2	4 h	55%
13	DMF	*t*-BuOK	2	O_2	4 h	68%
14	DMF	*t*-BuOK	4	O_2	4 h	85%
15	DMF	*t*-BuOK	5	O_2	4 h	88%
16	DMF	*t*-BuOK	3	O_2	3 h	85%
17	DMF	*t*-BuOK	3	O_2	2 h	82%
18	DMF	*t*-BuOK	3	O_2	1 h	84%
19	DMF	*t*-BuOK	3	Air	1 h	75%

[a] Reaction conditions: all reactions performed in a 20 mL scintillation *via*, **1a** (0.025 M), 2.5 mL of solvent, 4 Å-molecular sieves (MS), and room temperature (22 °C). All yields determined by ^{1}H NMR using internal standard.

While the difference was small for the sodium and potassium *tert*-butoxide salts (87% *vs.* 79% respectively), a noticeable difference in yield was observed between the K, Na, and Li hydroxides (55%, 31%, <1% respectively). Fewer than 3 equivalents of base (entry 12 and 13) were insufficient for the full consumption of the starting material. More than 3 equivalents of base (entry 14 and 15) were found to be unnecessary as there was no improvement in yield.

We then varied the reaction time (entry 16–18) and observed full consumption of starting material within one hour. Finally, when the reaction vial was charged with air instead of oxygen, **2a** was produced in 75% yield (entry 19). However, the rate of the reaction was slower and not all of **1a** was consumed.

We then explored the scope of substituents that are compatible with the reaction conditions. Variation in the pendant aryl ring revealed that heterocyclic substrates, as well as the substrates with *ortho*, *meta*, and *para* electron withdrawing groups produced the target products in good to excellent yields. On the other hand, electron donating groups were only tolerated in the *meta* position. Lower conversions to the corresponding isoindolinone were observed (39% and 48% respectively) for the reactions of 4-methoxy and 4-methyl substrates. However, substrate **2c** with a *para tert*-butyl group underwent the desired transformation in high yield (84%) (Table 2).

Substitution in the amide ring had a smaller effect – the reaction tolerated both electron donating and withdrawing groups, *ortho*, *meta*, and *para* to the amide. The overall transformation remained unaffected with halogens (*i.e.*, Br, Cl, and F) on either the amide ring or pendant aryl ring, allowing for the introduction of a useful synthetic handle for future modifications.

We also investigated the possibility of introducing additional substituents at the amide nitrogen. The *N*-methyl amide **2r** underwent the desired transformation sluggishly (30% yield, 74% based on reclaimed starting material) under the standard conditions. On the other hand, a *N*-methoxy amide remained unreactive under our standard conditions (*vide infra*).

Mechanistic studies

A series of studies designed to gain insight into the reaction mechanisms were performed and are listed below (Scheme 4). First, the C–H bond strength is critical for the reaction success. A BDE $\leq$ 85 kcal mol^{-1} was needed and simple benzylic or alkylbenzylic C–H bonds remained unreactive under our conditions (eqn (1)).

When the reaction is performed under an inert atmosphere (Ar), the consumption of **1a** is greatly diminished (eqn (2)), confirming the importance of O_2 as the oxidant.

Table 2 Amide scope for C(sp^3)–H amidation and hydroxylation[a]

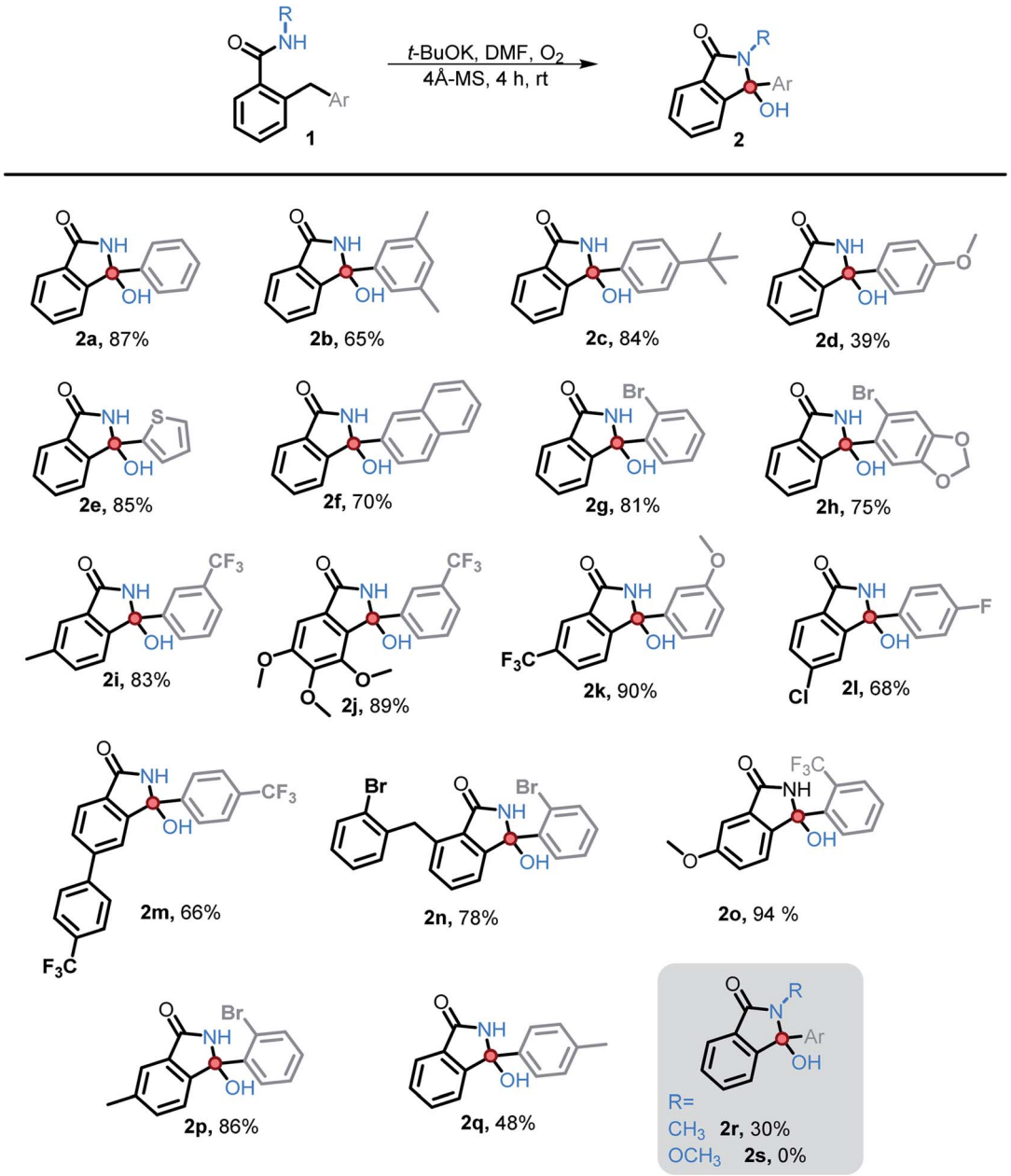

[a] Reaction conditions: benzamide (0.025 M), *t*-BuOK (3 eq.), 4 Å MS, DMF, O_2 balloon and the reactions were allowed to stir for 4 hours at rt. Unless stated otherwise, the yield is of the isolated product.

We have also considered the possible involvement of singlet oxygen. Singlet oxygen has been shown to be synthetically useful in the oxidation of heteroatoms, cyclization reactions, and the synthesis of hydroperoxides.[26] However, **1i** was fully consumed even in the absence of light, producing **2i** in 79% yield (eqn (3)). Reactivity in the dark indicates that singlet oxygen is not involved in the main path of this reaction.

Under these oxidative conditions, one could suggest that the reaction occurs *via* an oxidation of the CH_2 moiety to a carbonyl intermediate.[27] This intermediate could then close the cycle *via* nucleophilic attack of the amide onto the carbonyl under basic conditions. We have eliminated benzylic C–H oxidation in our early work by using *N*-Me substituted anilines, which yield products that clearly could not originate from the ketone.[10] Obtaining such direct evidence in the present case is problematic because, unlike the aniline cascade, the present amide cascade is terminated by C–O bond formation that renders the C/N radical–anion coupling and the carbonyl pathway products identical.

To test for the possible formation of a carbonyl intermediate, we wanted to use an unreactive amide in order to avoid the

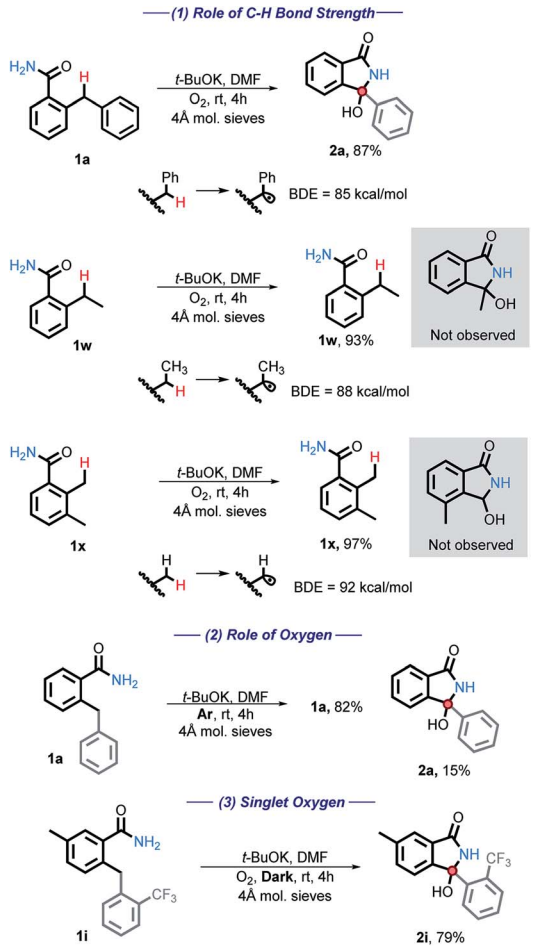

Scheme 4 Mechanistic tests for the C–H bond strength and for the participation of oxygen. All energies are reported in kcal mol^{-1}.

cyclization, while still allowing for the benzylic carbon to remain reactive enough to be oxidized into a ketone. However, no reaction was observed when amide **1s** was exposed to the standard conditions. Calculations show that if a ketone intermediate were formed, its cyclization would be thermodynamically favorable (ΔG = −5.1 kcal mol^{-1}). Assuming that this substitution at nitrogen does not directly change reactivity at the remote benzylic position, the lack of benzylic oxidation suggests that the carbonyl intermediate is not formed under our conditions[10] (Scheme 5). We have also found that an isoindolinone is readily converted into the respective 3-hydroxyisolindolinone under these conditions, a process that is unlikely to proceed through a carbonyl intermediate.

Computational data

Calculations were carried using the global-hybrid meta-GGA (U)M06-2X functional[28] and the 6-31+G(d,p) basis set for all atoms, with an ultrafine integration grid (99 590 points). A broken-spin approach was applied when necessary. The implicit SMD[29] solvation model was used to simulate the effects of *N*,*N*-dimethyl-formamide (DMF) throughout the calculated structures. Grimme's D3 version (zero damping) for empirical dispersion[30] was also included. Unless otherwise noted, all results presented are at the (SMD=DMF)/(U)M06-2X(D3)/6-31+G(d,p)/int=ufine level of theory. Frequency calculations were carried out for all structures to confirm them as either a minimum or a TS. All calculations were performed with the Gaussian 09 software package.[31] Three-dimensional depictions and orbital plots were produced with CYLView 1.0.1 [32] and Chemcraft 1.8.[33]

Radical cascade mechanism

Guided by these experimental results, we turned to computations for identifying the key intermediates of this transformation. A full thermodynamic landscape for the proposed reaction cascade is shown in Scheme 6. Each step in this cascade is thermodynamically favorable. In subsequent individual sections, we will discuss the individual steps along with their activation barriers and the respective experimental evidence.

Generation of DMF radical

We suggest that the chemical species responsible for the formation of the bis-benzylic C-centered radical is DMF radical ($C(O)N(CH_3)_2$). The formation of this radical under these conditions is well-documented. Yan *et al.* used them in a variety of interesting transformations that combined C–H activation and C–C bond formation.[34] However, the mechanism by which the DMF radical is generated is not fully established. A commonly suggested path that involves oxidation of DMF anion by DMF is highly thermodynamically unfavorable (ΔG = +54.0 kcal mol^{-1}, Scheme 7).[10]

While we were unable to find the pK_a of *t*-BuOH in DMF, literature reports[35] the pK_a of 1-butanol in DMF to be 33.3. It is reasonable to estimate the pK_a of *t*-BuOH in DMF to be *ca.* 34–35. The pK_a of DMF in DMF (38),[35] makes it approximately 3–4 pK_a units less acidic than *t*-BuOH. Although it makes the initial deprotonation of H–C(O)NMe_2 uphill, a small amount of DMF anion is still formed at equilibrium. Calculations show that although this deprotonation is endergonic by 11.2 kcal mol^{-1}, the activation barrier for the deprotonation of DMF is relatively low (12.6 kcal mol^{-1}, Scheme 7), and equilibrium should be reached quickly.

Indeed, Drapeau and co-workers noted a formamide proton shift, *via* ^{1}H and ^{13}C NMR, when *t*-BuOK was added to wet DMF-d_7.[36] Their computational work additionally highlighted two interesting points regarding the impact of counter ions. First, the cation stabilizes the DMF anion, assisting in deprotonation. Second, a cation of a certain size (*e.g.*, Li) can stabilize the DMF anion and increase the barrier for its oxidation to DMF radical.[36] Our experimental results also suggest that reaction is slow in the presence of Na and, to a greater extent, Li counterions (Table 1, entry 1, 7–10).

Our calculations show that the oxidation of DMF anion by oxygen is slightly exergonic (with the inclusion of K^+, Scheme 7). This makes the combined deprotonation and oxidation of DMF endergonic by ∼10 kcal mol^{-1}, which would allow only small quantities of DMF radical to be present at a given time. If the propagation step of the cascade is fast, then the initial penalty

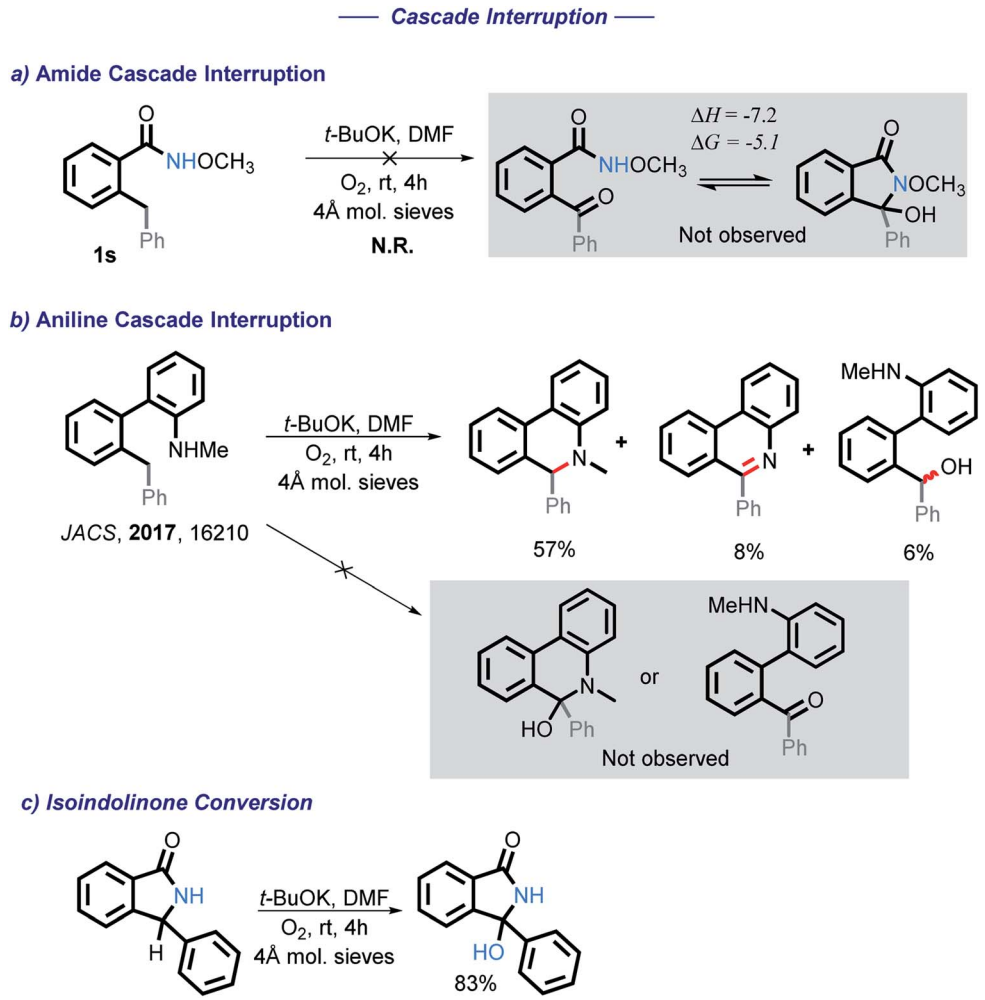

Scheme 5 Interruption of the amide and aniline cascades.

of forming the DMF radical is a small price to pay when all sequential steps in the cascade reactions are favorable and efficient. Overall, the generation of DMF radical imposes a ~10 kcal mol^{-1} penalty needed to initiate an otherwise exergonic sequence. Interestingly, calculations suggest that the activation barrier for proton abstraction from DMF is almost

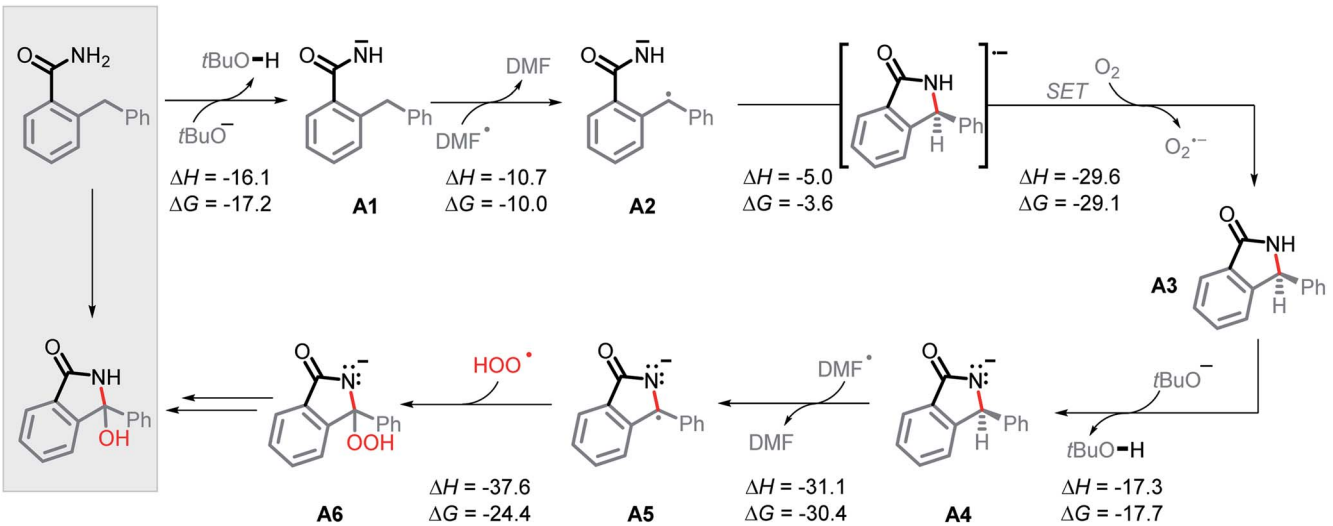

Scheme 6 Proposed mechanism and calculated reaction thermodynamics for the individual steps in the N–H/C–H amidation. All energies are in kcal mol^{-1}.

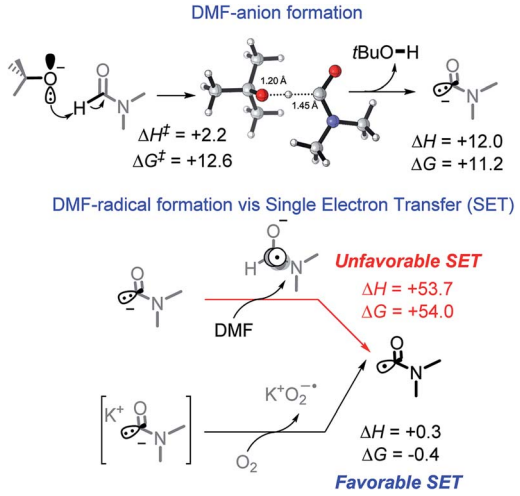

Scheme 7 Formation of DMF radical. All energies reported in kcal mol^{-1}.

entirely entropic (enthalpy of activation is only 2.2 kcal mol^{-1}). The TS Gibbs energy (12.6 kcal mol^{-1}) is only 1.4 kcal mol^{-1} higher than the Gibbs energy of the product, suggesting that the deprotonation should be rapidly reversible.

Deprotonation/H-atom transfer

The unusual nature of our intramolecular C–H amination stems from the generation of a radical and an anion *in situ*. To achieve this, two criteria must be met. First, an acidic proton is needed for a deprotonation that produces a persistent N-anion. Second, the substrates should have a sufficiently weak C–H bond that undergoes HAT with the formation of a C-radical.

The cascade mechanism begins with the exergonic deprotonation of the mildly acidic benzamide by *tert*-butoxide ($\Delta G = -17.2$ kcal mol^{-1}, Scheme 6, **A1**). Once a persistent nitrogen anion is quickly generated, the slowly produced DMF radical (see the ESI† for discussion of DMF radical formation) can engage the sufficiently weak bis-benzylic C–H bond (BDE = 85 kcal mol^{-1}) in a HAT step ($\Delta G = -10.0$ kcal mol^{-1}, Scheme 6, **A2**). This step yields the initial acyclic radical–anion intermediate. While the HAT $\Delta G^{\ddagger}$ and ΔG are slightly lower for the neutral amide than the deprotonated amide ($\Delta G^{\ddagger} = 17.6$ *vs.* 19.1, $\Delta G = -10.9$ *vs.* -10.0 kcal mol^{-1}), the high concentration of base and the highly favorable thermodynamics for the deprotonation step should result in the majority of HAT occurring after deprotonation (Scheme 8).

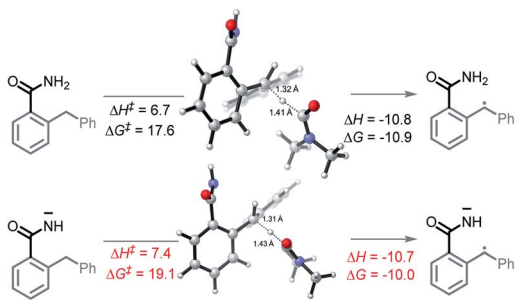

Scheme 8 Reaction energy profiles and twisted transition states for C–H activation in neutral and deprotonated substrates. All energies are in kcal mol^{-1}.

While *tert*-butoxide can deprotonate the benzylic C–H bond of diphenylmethane[37] (pK_a = 32.2 in DMSO), the benzamide's N–H bond is far more acidic (pK_a = 23.3 in DMSO). The nine orders of magnitude difference in acidity leaves no doubt that the N–H bond should be deprotonated preferentially. In our previous work, we explored the possibility of *t*-BuOK deprotonating the benzylic C–H bond and found that ΔG for this process is also favorable (-3 kcal mol^{-1}) suggesting that C–H deprotonation is feasible as well. However, once the initial nitrogen anion is formed, the second deprotonation would form a dianion. Although the possibility of a dianionic process cannot be completely eliminated at the present stage, we favor the radical HAT path for the C–H activation because of the coulombic penalty associated with the formation of multiply charged species.

The transition state for the initial HAT is interesting. At the stage where the benzylic C–H bond begins to break to form the C-centered radical, the benzylic C–H is *misaligned* with the aromatic π-system. Hence, the forming radical finds itself in alignment only with the pendant aromatic ring. One might expect that as this radical would prefer to be in a close alignment with both aromatic rings to take advantage of stereoelectronic stabilization. This finding explains why the pendant aryl group is necessary – although the CH_2 groups in substrates **1w** and **1x** are formally "benzylic" (Scheme 4), the core aryl group does not directly contribute to their C–H activation. Under these intramolecular stereoelectronic constraints, their relatively low BDE values are somewhat misleading.

Furthermore, the amide is rotated out of conjugation the aromatic π-system in a nearly orthogonal geometry.[38] The twisted geometry may provide an explanation to why amide deprotonation does not activate the *ortho*-benzylic C–H bond towards H-abstraction. Steric hindrance between the two relatively large *ortho*-substituents contributes to this geometric preference. On the other hand, the amide π-system may engage in through-space interactions with the back lobe of the antibonding orbital of the breaking C–H bond. In this scenario, the amide may be assisting in the C–H activation process by helping to stabilize the newly forming radical *via* a through-space interaction.

Radical–anionic cyclization and C–N bond formation

In the key step of the overall cascade, the N-anion and the C-centered radical in **A2** react to form a 2c,3e "half" bond, also making a cyclic radical–anion in the process. Interestingly, this process occurs without the apparent loss of amide resonance since it is the 2nd "in-plane" lone pair of nitrogen that is involved in the N–C coupling. On the other hand, the radical center rotates out of conjugation with the central aryl ring as well. The latter stereoelectronic penalty is likely to contribute to a relatively high, 17.2 kcal mol^{-1}, Gibbs barrier and the low thermodynamic driving force, $\Delta G = -3.6$ kcal mol^{-1}, for this

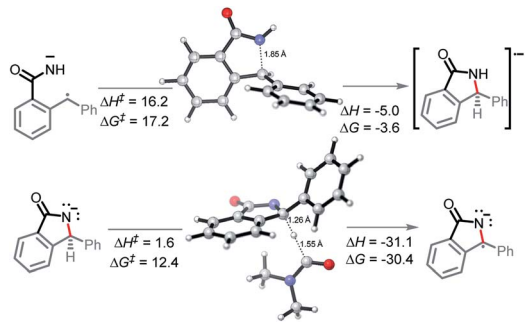

Scheme 9 Transition states for the C–N bond formation and second HAT.

seemingly trivial step (Scheme 9). These values are significantly less favorable than the analogous values for the C–N bond formation from deprotonated anilines (8.5 and −27.8 kcal mol^{-1}, respectively) reported in our earlier work. This dramatic difference highlights the importance of N-partner basicity/donor ability for this process. We will discuss this factor further in the conclusions section of this manuscript.

Additionally, the three non-bonding electrons of the radical and anion reacting partners have to find "a new home" in this step. Two of these electrons are accommodated in the newly formed σ orbital of the C–N bond. The third electron avoids its apparent destiny of ending up at the high energy σ^*_{C-N} orbital by "hopping" to a lower energy π* orbital of the aromatic ring (Scheme 10). This state crossing, not unusual for radical-anionic reactions,[39] stabilizes the product by creating a delocalized π-type radical–anion.

Nevertheless, the reacting system evolved from a mild reductant (electron in a non-bonding orbital) into a more potent reductant (electron is an antibonding orbital). The high reducing power of the cyclic product allows its reaction with a mild oxidant, such as molecular oxygen. This reaction (*i.e.*, single electron transfer) removes the antibonding electron, converting a 2c,3e-bond into a normal 2c,2e C–N bond. This step simultaneously forms superoxide in a thermodynamically favorable way with $\Delta G = -29.1$ kcal mol^{-1} (Scheme 6, **A3**).

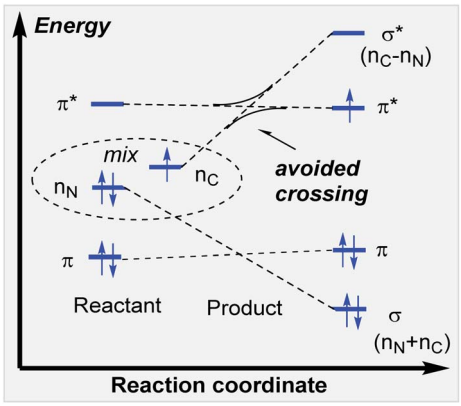

Scheme 10 State crossing avoids populating the high energy σ^*_{C-N} orbital.

After the benzamide is cyclized into an isoindolinone, the cyclic intermediate is deprotonated to give anion **A4** (Scheme 6, $\Delta G = -17.7$ kcal mol^{-1}). The α-C–H bond in this anion is sufficiently weakened to form a stabilized radical–anion **A5** ($\Delta G = -30.4$ kcal mol^{-1} after a HAT to DMF radical).

Diverting from C=N to C–O bond formation

From the stabilized radical intermediate **A5**, one can envision two possible mechanisms for the formation of the C–O bond (Scheme 11). The first is similar to what we reported in our previous work,[10] in which the intermediate is oxidized a second time by molecular oxygen to form the C=N moiety of an imine intermediate. This intermediate may then be intercepted by a suitable nucleophile generated *in situ*, such as superoxide or hydroxide. In particular, superoxide is known to undergo disproportionation to give O_2 and hydroxide under aqueous conditions.[40] It is possible that a similar process to generate hydroxide could occur under the conditions of our C–H amination reaction, whereas *t*-BuOH would serve as the proton source instead of H_2O. The second possibility, is that a radical coupling partner such as superoxide or hydroperoxyl radical couples to the C-centered radical making a hydroperoxide intermediate.

We initially tested to see if the addition of an external nucleophile could be used to trap the plausible imine intermediate. The addition of either sodium or potassium

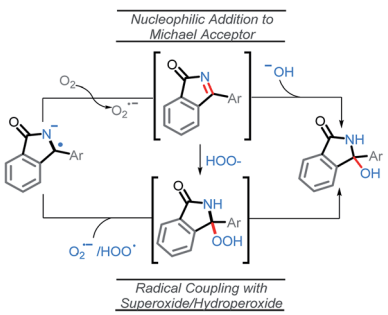

Scheme 11 Possible routes to product from stabilized radical–anion intermediate.

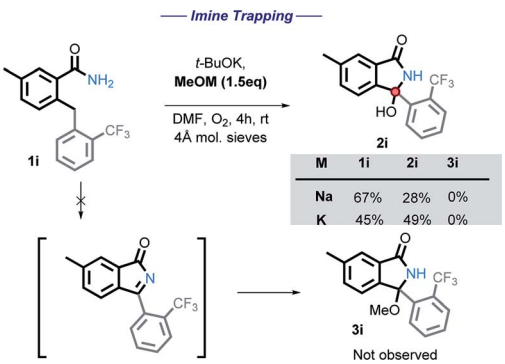

Scheme 12 Attempting to trap the hypothetical imine intermediate.

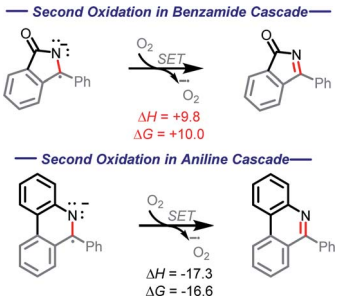

Scheme 13 Contrasting thermodynamics (kcal mol^{-1}) for the C=N forming oxidations in the amide and aniline cascades.

methoxide hinders the reaction, with no methoxy product observed in these experiments (Scheme 12).

Our calculations show the oxidation of radical–anion **A5** by O_2 is thermodynamically uphill (ΔG = +10.0 kcal mol^{-1}, Scheme 13). While this is not a prohibitive price to pay, it is worth noting that this oxidation step is 39.1 kcal mol^{-1} more endergonic than the initial oxidation step. This substantial increase stems from several factors, including lack of aromatic stabilization in the N-heterocyclic part of the product as well as the additional radical and charge stabilization in the reactant, not only through the bis-phenyl groups, but additionally through the nitrogen and carbonyl.

This finding contrasts our previous work with anilines where the second oxidation step was favorable (ΔG = −16.6 kcal mol^{-1}) due to the formation of an aromatic system.[10] In the present case, the situation is different, and this differences manifests itself in a divergent reaction pathway (formation of a C–O bond instead of C=N moiety). To understand this step better, we explored the possibility of radical coupling being responsible for the final C–O formation.

A series of studies designed to gain insight into the possible radical coupling of **A5** were performed and are listed below (Scheme 14).

We then employed two common radical trapping agents, attempting to either trap a radical intermediate or to inhibit the reaction. TEMPO, caused a slight decrease in isolated yield (87% *vs.* 76%) but no TEMPO trapped product or recovered starting material was observed (eqn (1)). This finding is consistent with the radical mechanism if intramolecular radical trapping (*i.e.*, the cyclization) is faster than the intermolecular trapping, or if TEMPO can play an alternative role by promoting the C–H activation step. More detailed discussion on the possible role of TEMPO will be given in a subsequent section.

We also tested the effect of a common radical and peroxide trapping agent, 3,5-di-*tert*-4-butylhydroxytoluene (BHT), at the standard reaction conditions (eqn (2)). The phenol moiety of BHT is often used to halt the autoxidation of organic molecules with oxygen, analogous to that of vitamin E. BHT can deactivate two (usually peroxy) radicals – the first one by a hydrogen atom transfer and the second one by reaction at the cycle.[41]

We found that the reaction is partially inhibited – **2i** was isolated in a 47% yield, starting material recovered in 27% isolated yield. Furthermore, BHT-OH was additionally isolated in 25% yield. Low yields are a result of isolation difficulties. Formation of this product further suggests that a radical pathway is involved.

Addition of superoxide/hydroperoxyl radical to the radical–anion A5

It is unlikely that the OH group in the final product is a result of radical coupling with hydroxide radical, as it is highly reactive and will likely abstract a hydrogen atom from the solvent or *t*-BuOH before reaching the reactant.[42] This consideration led us to explore the possibility of radical

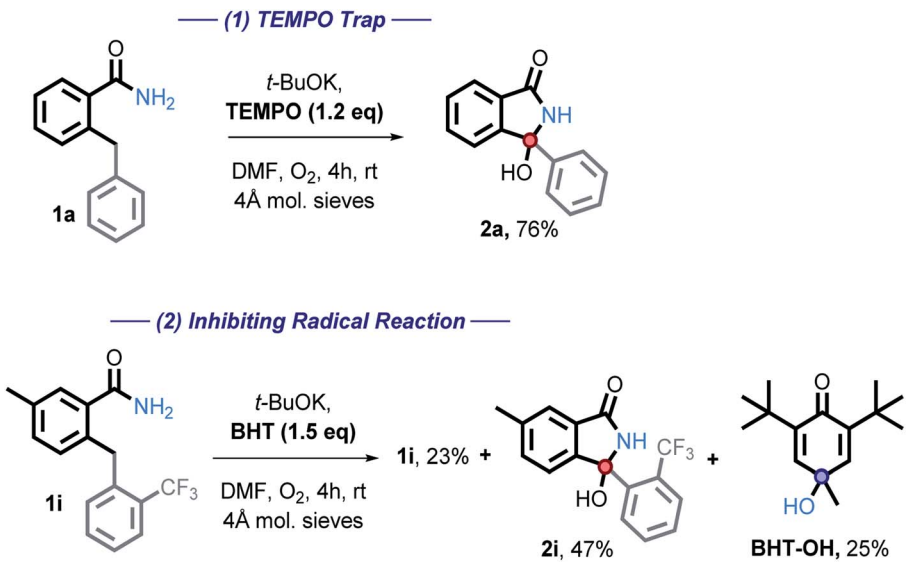

Scheme 14 Radical coupling mechanistic studies.

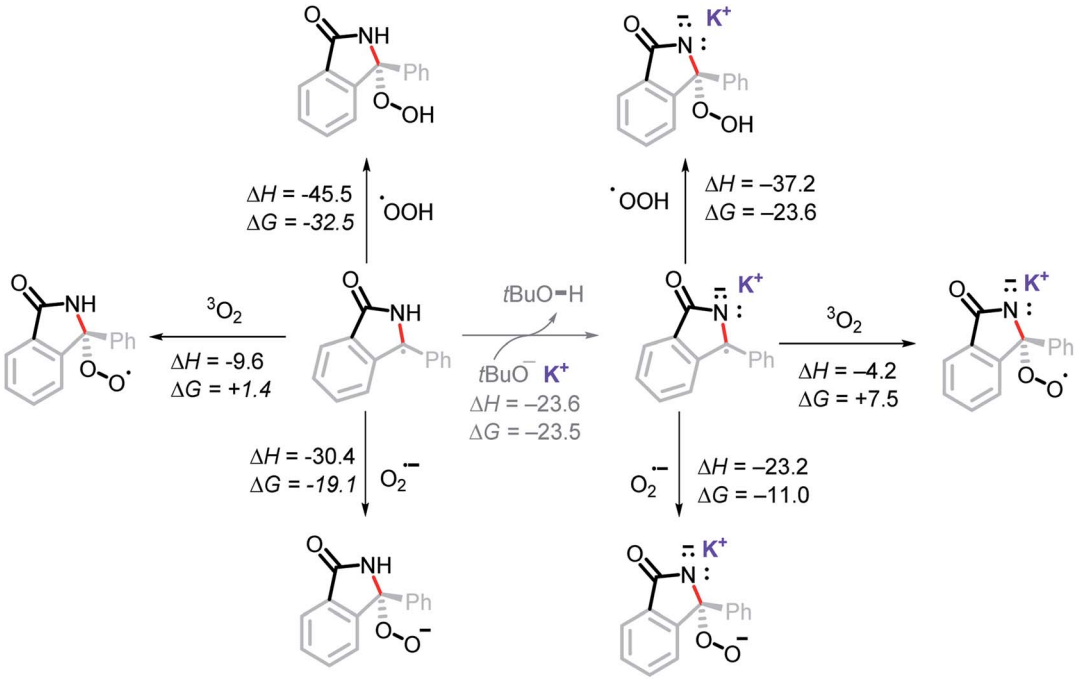

Scheme 15 Computational thermodynamic data for the addition of molecular oxygen, superoxide, and hydroperoxyl radical to the stabilized radical intermediate. Energies in kcal mol^{-1}.

coupling with superoxide or with its conjugate acid, the hydroperoxyl radical (HOO•).[43]

Our calculations show this to be a favorable path for forming the C–O bond (Scheme 15). In particular, radical addition to intermediate **A5** *via* HOO• was found to be highly exergonic, $\Delta G = -23.6$ kcal mol^{-1}. Addition of superoxide (the precursor of HOO•) to **A5** was favorable, $\Delta G = -11.0$ kcal mol^{-1}. On the other hand, the addition of molecular oxygen was found to be endergonic, $\Delta G = +7.5$ kcal mol^{-1}. It is worth noting that all three of these proposed pathways are thermodynamically more favorable than an oxidation of **A5** by O_2 ($\Delta G = +10.0$ kcal mol^{-1}).

Superoxide has been shown to act as a Brønsted base in aprotic media and deprotonate weak acids such as 1-butanol in DMF (pK_a = 33.3 in DMF).[44] It is therefore possible, that superoxide may deprotonate *t*-BuOH (estimated p$K_a \approx$ 34–35 in DMF) generated *in situ*, forming HOO•. Hence, both HOO• and superoxide may couple with **A5**.

The evidence that we have presented up to this point suggests that formation of a hydroperoxide intermediate[45] should be considered (Scheme 6, **A6**). To explore this possibility, we prepared this intermediate and tested its properties as described in the following section.

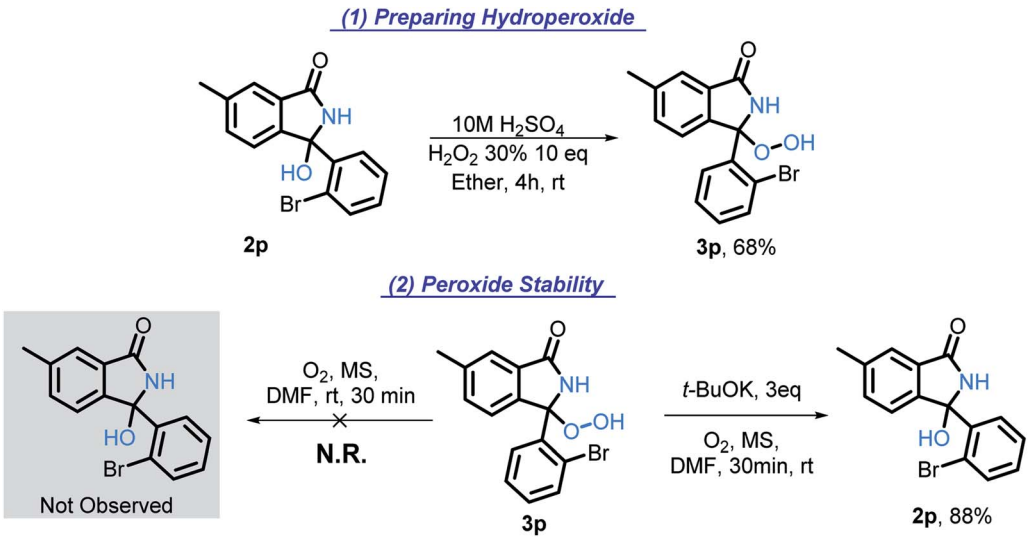

Scheme 16 Preparation and instability of the suggested hydroperoxide intermediate.

Hydroperoxide intermediate

The hydroxy group of **2p** was converted into hydroperoxy group of **3p** (Scheme 16, eqn (1)) by acid-catalyzed reaction with H_2O_2. The reference spectra contained the characteristic broad downshifted peak of a hydroperoxide that readily underwent deuterium exchange.[46] After subjecting **3p** to our standard conditions, the formation of **2p** was observed by TLC within five minutes. In half an hour, **2p** was formed in 88% yield (Scheme 16, eqn (2)). The lack of **3p** reactivity in the absence of *t*-BuOK (Scheme 16, eqn (2)) indicates the important role of *t*-BuOK in the reduction of the hydroperoxide intermediate into the final product.

Because of the rapid consumption of hydroperoxide in the presence of base, we anticipate its existence *in situ* to be fleeting. The existence of transient hydroperoxide intermediates, that convert to OH-bearing final products, has previously been reported in O_2-mediated oxidations of C(sp^3)–H bonds.[47] Indeed, in several experiments, ^{1}H NMR of the reaction mixtures showed a broad downshifted singlet, potentially indicative of the hydroperoxide, (see ESI for additional details†). Although this intermediate was too unstable to persist and to be reliably detected under the reaction conditions, these findings suggest that a hydroperoxide intermediate (Scheme 6, **A6**) is formed transiently and reduced by *t*-BuOK/*t*-BuOH into the final isoindolinone product. The hydroperoxide may also be involved in the radical chain propagation by serving as a possible source of O-centered radicals that can assist in the C–H activation step.

Secondary amides

We were intrigued by the sluggish reactivity of the secondary amides. Since we isolate unreacted starting material, the reaction is interrupted in the initial stages. Yet our calculations find that each of the three initiation steps, *i.e.*, the deprotonation ($\Delta G = -16.0$), HAT ($\Delta G = -9.3$), and the radical–anion cyclization ($\Delta G = -5.9$), for **1r** are thermodynamically favorable (Scheme 17).

We used computed activation barriers to understand why the secondary amides are unreactive (see ESI†). Our analysis suggests that the barrier for the H-abstraction is about 1.2 kcal mol^{-1} higher for the secondary amides than it is for the primary amides. This difference should lead to a *ca.* 10-fold rate decrease for this step, providing a possible explanation for the low reactivity of the secondary amide substrates under the reaction conditions.

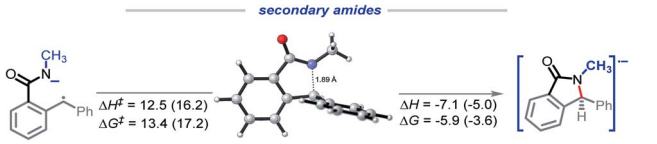

Scheme 18 Computed activation and reaction enthalpies and Gibbs energies for the cyclization of secondary amide **1r**. Numbers in parentheses are for primary amide **1a**. All numbers reported in kcal mol^{-1}.

Conversely, the calculated barrier for the C–N bond formation is *lower* for the secondary amides, indicating that this step is unlikely to be the cascade bottleneck (Scheme 18). Aimed by these observation, we have concentrated our attention on the H-transfer step.

Indeed, focus on C–H activation allowed us to solve the problem of secondary amides as described below. Recalling that TEMPO had no detrimental effect on our radical reaction, we considered the possibility of TEMPO assisting in C–H activation.

Indeed, literature suggests that TEMPO can be a useful additive to the oxidation of benzylic C(sp^3)–H bonds. For example, TEMPO can be oxidized into an oxoammonium salt (TEMPO+) in the presence of hydroperoxyl radical, peroxyl

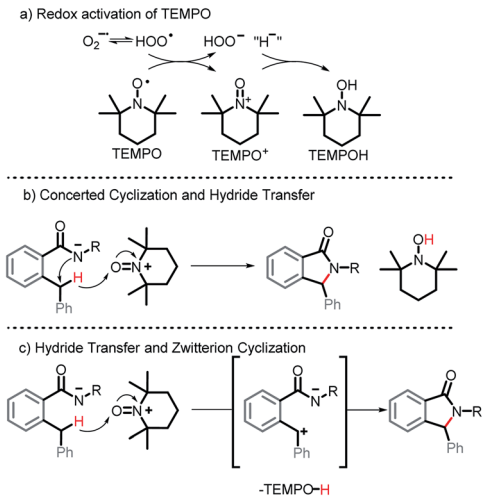

Scheme 19 Potential pathways for TEMPO assistance in C–H activation.

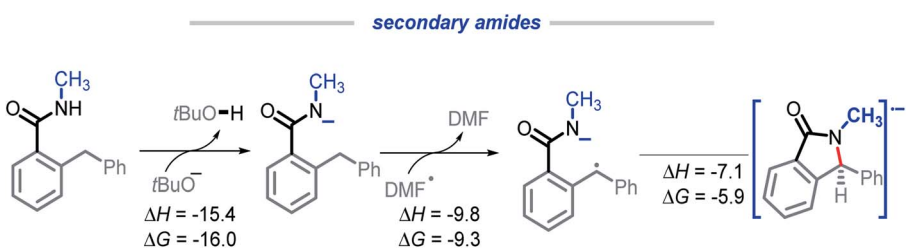

Scheme 17 Calculations for the deprotonation, HAT, and radical–anion cyclization of **1r**. All energies are reported in kcal mol^{-1}.

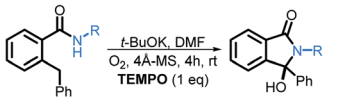

Substrate	Product	Yield, %
1r	2r	30[a], 74[b], 86[c]
1s	2s	0[a], 31[b], 94[c]
1t	2t	49[a], 87[b], 87
1u	2u	33[a], 54[b], 71[c]
1v	2v	25[a], 55[b], 87[c]

Scheme 20 Improved C–H activation with TEMPO as an additive. Reaction conditions: secondary benzamide (0.025 M), *t*-BuOK (3 eq.), DMF (2 mL), 4 Å MS, O_2 balloon, reactions stirred at r.t. overnight. [a]Isolated yields for reaction performed under standard conditions. [b]Isolated yields for reactions with the addition of TEMPO. [c]Yields based of reclaimed starting materials with the addition TEMPO.

radicals, or a secondary oxidant (*e.g.* NaOCl) as shown in Scheme 19a.[48] The latter has been shown to act as an oxidant that may facilitate the forward progression of redox reactions.[49] In particular, TEMPO+, generated *in situ*, from TEMPO was used as a cocatalyst in the aerobic oxidation of benzylic C(sp^3)–H into carbonyls.[50] Even if the carbonyl intermediate is formed in this case, it would, as we previously discussed in Scheme 5, readily cyclize under basic conditions into our isoindolinone product.

Additionally, TEMPO+ has been suggested to facilitate benzylic hydride transfers.[51] It is plausible that in our case, a concerted C–N bond formation and benzylic hydride transfer to TEMPO+ occurs generating TEMPOH and our cyclized product (Scheme 19b). Alternatively, one can consider a hydride transfer to TEMPO+ forming a benzylic carbocation that is immediately trapped intramolecularly *via* cyclization (Scheme 19c).

Although the exact mechanistic path for C–H activation in our system is so far unknown, the combination of possible attractive scenarios motivated us to test the effect of TEMPO on the reaction. To our delight, we observed the nearly full consumption when secondary amide **1r** was subjected to the optimized conditions along with TEMPO. Interestingly, no TEMPO-trapping product was present in the reaction mixture. Instead, **2r** was obtained in 74% isolated yield a dramatic improvement over the standard conditions (30% without TEMPO *vs.* 74% with TEMPO, Scheme 20). Motivated by this finding, we tested reactivity of **1s** in the presence of TEMPO. Gratifyingly, the reaction affords **2s**, albeit in a moderate yield of 31% (the majority of reaction mixture is unreacted **1s**). Furthermore, substrates **1t**, **1u**, and **1v** also showed a substantial increase in reactivity with the addition of TEMPO and the products **2t**, **2u**, and **2v** were isolated in 87%, 54%, and 55% respectively.

Nitriles

As we explored the reactivity of amides under our oxidative C–H amination conditions, we decided to take advantage of the electrophilic nature of benzonitriles, a common precursor in our amide synthesis. In the presence of a suitable nucleophile, anionic addition to the electrophilic carbon on nitriles will result in formation of a nitrogen anion. This anion may then trap a carbon radical, forming a C–N bond upon oxidation.

Indeed, nitrile **4a** was found to transform into **2a** in good yield (72%) in the presence of *t*-BuOK and O_2 in DMF (Scheme 21). Two interesting side products were isolated as well. The rearranged product **5a** is a result of C–H and C–C activation. Because product **6a** was not reported previously, we have confirmed its structure by single crystal X-ray crystallography (see ESI†). Although the mechanism and scope of these transformations will have to be explored further in the future work, this finding does illustrate that the scope of the present approach to C–H activation extends beyond amide and aniline couplings.

Conclusion

We have developed a direct non-photochemical method for converting C(sp^3)–H bonds into C–N and C–O bonds under mild conditions with the aid of base, molecular oxygen, and DMF. Each component of the overall reaction plays a pivotal role in a coordinated sequence of deprotonation, H-atom transfer, and electron transfer that forges the C–N bond. The base has three main functions: (1) to deprotonate the N–H bond, (2) to provide an adequate concentration of DMF carbamoyl anion to be converted to DMF radical, and (3) to convert the hydroperoxide intermediate into the final hydroxyl product. The DMF radical performs selective HAT at the di-benzylic C(sp^3)–H to form a C-centered radical. The C–N bond is formed initially through a 2c,3e interaction between the N-anion and C-radical. Oxidation of the radical–anion intermediate by oxygen completes the C–N bond forming sequence. Computational data suggest that the stabilized radical anion formed after the second HAT could not be oxidized by molecular oxygen. Instead, the radical couples with either superoxide or hydroperoxide species to generate a hydroperoxide intermediate that ultimately

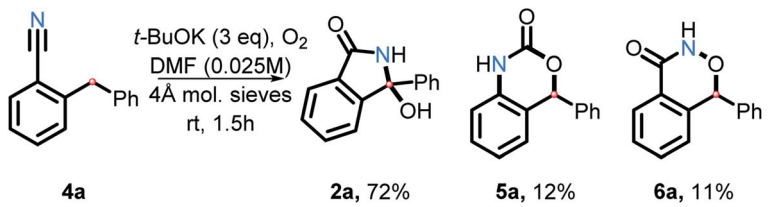

4a **2a**, 72% **5a**, 12% **6a**, 11%

Scheme 21 C–H activation and cyclization of a nitrile substrate.

decomposes to form the hydroxide product. Addition of TEMPO opens the door for the use of secondary amides and improves the performance of some insufficiently reactive primary amides. This process allows for the formation of functionalized N-heterocycles in an operationally simple and robust fashion.

Importantly, this work dramatically expands the range of N-anions that can participate in the three-electron approach to C–N bond formation. In general, 2c,3e-bonds are weaker than their classic 2c,2e-counterparts. Hence, limitations for their formation are much more severe. For example, the C–N bond formation in the radical cyclization with anilines is uphill by >20 kcal mol^{-1}. One of the reasons why this deceivingly simple transformation is unfavorable is that it leads to the development of cationic character at nitrogen. Trading the lone pair of nitrogen for a 2c,3e-bond removes electron density from the N atom – an "oxidation" process that this electronegative element generally resists. Making nitrogen more electron rich, preferably anionic, is key to overcoming this problem.[10]

In the present work, we have increased N–H bond acidity by seven orders of magnitude from our earlier studies by switching from anilines[10] (pK_a ~ 30 in DMSO) to amides (pK_a ~ 23 in DMSO). Such deactivation of the conjugated nitrogen base increases the activation barrier for C–N bond formation from 8.5[10] to 17.2 kcal mol^{-1} and decreased reaction exergonicity from 28[10] to 4 kcal mol^{-1}. Thus, the present use of a stabilized N-anion provided important "bracketing" information on the thermodynamic limits of three-electron C–N bond formation. Although the initial correlations presented in Scheme 22 are crude, considering the small number of points and differences in the formed ring size, they should provide the first approximate guidelines for the design of such reactions.

Furthermore, even though the C–N bond formation from deprotonated benzamides is still efficient despite the additional kinetic and thermodynamic penalties, the next step, *i.e.*, the C=N moiety formation, is not favorable anymore! Here, the cyclized radical–anion is so stable that it does not undergo one-electron oxidation under the reaction conditions. Instead, a new reactivity pattern becomes available and the reaction sequence culminates in the formation of a C–O bond instead of a C=N moiety.

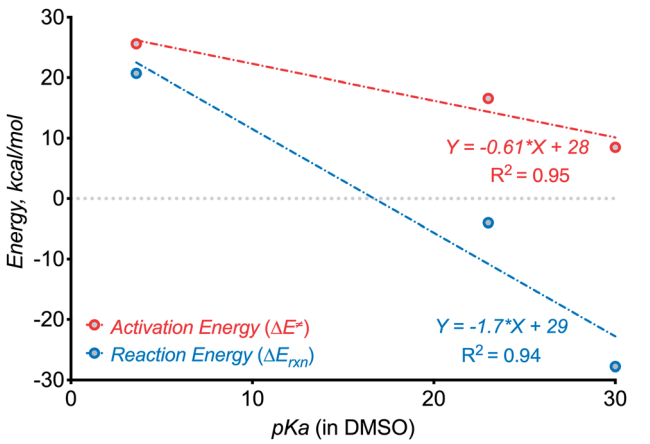

Scheme 22 Testing for the effect of N–H component acidity on the kinetics and thermodynamics of three-electron C–N bond formation.

These observations can guide the choice of N–H components in future reactions that form 2c,3e bonds. There is a broad range (pK_a ~ 20–32 in DMSO) of N–H bonds that can be deprotonated by potassium *tert*-butoxide but do not form an overstabilized and unreactive conjugate base. For such N–H partners, a variety of possible C–H bonds may be used for generating a suitable C-radical for the three-electron C–H aminations. One can sufficiently weaken the C–H bond (BDEs in the range of 80–90 kcal mol^{-1}) by placing heteroatoms or non-aromatic π-systems next to the methylene carbon.

The *N*-deprotonated benzamides presented in this work are close to the "pK_a limit" for three-electron bond formation from benzylic radicals. In order to expand this limit to less reactive, more stabilized nitrogen bases, one has to use more reactive, less stabilized radical partners. We hope that our report will encourage broad investigation of new strategies for unconventional C–N bond formation.

Conflicts of interest

The authors declare no conflicts of interest.

Acknowledgements

The fundamental and synthetic aspects of this study were supported by donors of the ACS Petroleum Research Fund (PRF#57377-ND4) and by the National Science Foundation (CHE-1465142). We appreciate the allocation of computational resources from FSU RCC and the NSF XSEDE (TG-CHE160006) and assistance in acquiring ^{1}H and ^{13}C NMR spectra from the NMR Facility of FSU Department of Chemistry and Biochemistry. G. P. G. is grateful to Professor Alán Aspuru-Guzik (University of Toronto) for his support.

References

1 (*a*) J. Wencel-Delord and F. Glorius, *Nat. Chem.*, 2013, **5**, 369–375; (*b*) Q. Lu and F. Glorius, *Angew. Chem., Int. Ed.*, 2017, **56**, 49–51; (*c*) G. Choi, Q. Zhu, D. C. Miller, C. Gu and R. R. Knowles, *Nature*, 2016, **539**, 268–271; (*d*) J. C. K. Chu and T. Rovis, *Nature*, 2016, **539**, 272–275; (*e*) M. S. Burg, M. Gicquel, S. Breitenlechner and A. Pöthig, *Angew. Chem., Int. Ed.*, 2018, **57**, 2953–2957; (*f*) J. K. Chu and T. Rovis, *Angew. Chem., Int. Ed.*, 2018, **57**, 62–101.

2 (*a*) B. Peng and N. Maulide, *Chem.–Eur. J.*, 2013, **19**, 13274–13287; (*b*) J. Xie, C. Pan, A. Abdukader and C. Zhu, *Chem. Soc. Rev.*, 2014, **43**, 5245–5256; (*c*) Y. Park, Y. Kim and S. Chang, *Chem. Rev.*, 2017, **117**, 9247–9301; (*d*) P. Thansandote and M. Lautens, *Chem.–Eur. J.*, 2009, **15**, 5874–5883.

3 (*a*) M. S. Chen and C. White, *Science*, 2010, **327**, 566–571; (*b*) S. Murahuashi, N. Komiya and T. Nake, *J. Am. Chem. Soc.*, 2003, **125**, 15312–15313; (*c*) B. Dangel, K. Godula, S. Won Youn, B. Sezen and D. Sames, *J. Am. Chem. Soc.*, 2002, **124**, 11856–11857; (*d*) D. Shabashov and O. Daugulis, *J. Am. Chem. Soc.*, 2010, **132**, 3965–3972; (*e*) O. V. Zatolochnaya and V. Gevorgyan, *Nat. Chem.*, 2014, **6**, 661–663; (*f*)

Y. N. Timsina, B. F. Gupton and K. C. Ellis, *ACS Catal.*, 2018, **8**, 5732–5776; (*g*) A. Dhakshinamoorthy, A. Asiri and H. Garcia, *ACS Catal.*, 2019, **9**, 1081–1102; (*h*) Z. Zhou and L. Kürti, *Synlett*, 2019, **30**, 1525–1535.

4 (*a*) D. Hazelard, P. Nocquet and P. Compain, *Org. Chem. Front.*, 2017, **4**, 2500–2521; (*b*) F. Collet, R. H. Dodd and P. Dauban, *Chem. Commun.*, 2009, **34**, 5061–5074; (*c*) T. A. Ramirez, B. Zhao and Y. Shi, *Chem. Soc. Rev.*, 2012, **41**, 921–942; (*d*) W. R. Gutekunst and P. S. Baran, *Chem. Soc. Rev.*, 2011, **40**, 1976–1991; (*e*) J. L. Jeffrey and R. Sarpong, *Chem. Sci.*, 2013, **4**, 4092–4106.

5 (*a*) A. Arai, Y. Ueda, K. Morisaki, T. Furuta, T. Sasamori, N. Tokitoh and T. Kawabata, *Chem. Commun.*, 2018, **54**, 2264–2267; (*b*) M. Kono, S. Harada and T. Nemoto, *Chem.–Eur. J.*, 2017, **23**, 7428–7432; (*c*) M. Rauser, C. Ascheberg and M. Niggemann, *Angew. Chem., Int. Ed.*, 2017, **56**, 11570–11574; (*d*) P. Starkov, T. F. Jamison and I. Marek, *Chem.–Eur. J.*, 2015, **21**, 5278–5300; (*e*) T. A. Ramierez, B. Zhao and Y. Shi, *Chem. Soc. Rev.*, 2012, **41**, 931–942; (*f*) F. Collet, C. Lescot and P. Dauban, *Chem. Soc. Rev.*, 2011, **40**, 1926–1936; (*g*) J. D. Bois, *Org. Process Res. Dev.*, 2011, **15**, 758–762; (*h*) J. B. Aguila, Y. M. Badiei and T. H. Warren, *J. Am. Chem. Soc.*, 2013, **135**, 9399–9406; (*i*) X. Zhang, H. Xu, X. Liu, D. L. Phillips and C. Zhao, *Chem.–Eur. J.*, 2016, **22**, 7288–7297.

6 (*a*) X. Hu, X. Qi, J. Chen, Q. Zhao, Q. Wei, Y. Lan and W. Xia, *Nat. Commun.*, 2016, **7**, 11188–11200; (*b*) K. C. Nicolaou, P. S. Baran, Y.-L. Zhong, S. Barluenga, K. W. Hunt, R. Kranich and J. A. Vega, Iodine, *J. Am. Chem. Soc.*, 2002, **124**, 2233–2244; (*c*) Y. Wang, H. Chen, X. Zhu and S. Chiba, *J. Am. Chem. Soc.*, 2012, **134**, 11980–11983; (*d*) G. Cecere, C. M. König, J. L. Alleva and D. W. C. MacMillan, *J. Am. Chem. Soc.*, 2013, **135**, 11521–11524; (*e*) L. J. Allen, P. J. Cabrera, M. Lee and M. S. Sanford, *J. Am. Chem. Soc.*, 2014, **136**, 5607–5610; (*f*) K. T. Tranatino, D. C. Miller, T. A. Callon and R. R. Knowles, *J. Am. Chem. Soc.*, 2015, **137**, 6440–6443.

7 (*a*) A. W. Hofmann, *Ber. Dtsch. Chem. Ges.*, 1879, **12**, 984–990; (*b*) M. Wolff, *Chem. Rev.*, 1963, **63**, 55–64.

8 (*a*) J. B. McManus, N. P. R. Onuska and D. A. Nicewicz, *J. Am. Chem. Soc.*, 2018, **140**, 9056–9060; (*b*) K. A. Margrey, A. Leven and D. A. Nicewicz, *Angew. Chem., Int. Ed.*, 2017, **56**, 15644–15648; (*c*) M. H. Shaw, V. W. Shurtleff, J. A. Terrett, J. D. Cuthbertson and D. W. C. MacMillan, *Science*, 2016, **352**, 1304–1308; (*d*) J. L. Jeffrey, F. R. Petronijević and D. W. C. MacMillan, *J. Am. Chem. Soc.*, 2015, **137**, 8404–8407; (*e*) C. K. Prier and D. W. C. MacMillan, *Chem. Sci.*, 2014, **5**, 4173–4178; (*f*) H. Bartling, A. Eisenhofer, B. König and R. M. Gschwind, *J. Am. Chem. Soc.*, 2016, **138**, 11860–11871.

9 C. J. Evoniuk, S. P. Hill, K. Hanson and I. V. Alabugin, *Chem. Commun.*, 2016, **52**, 7138–7141.

10 C. J. Evoniuk, G. P. Gomes, S. Hill, F. Satoshi, K. Hanson and I. V. Alabugin, *J. Am. Chem. Soc.*, 2017, **139**, 16210–16221.

11 (*a*) M. Yang, B. Su, Y. Wang, K. Chen, X. Jiang, Y. Zhang, X. Zhang, G. Chen, Y. Cheng, Z. Cao, Q. Guo, L. Wang and Z. Shi, *Nat. Commun.*, 2014, **5**, 4707–4713; (*b*) Y. Timsina, F. Gupton and K. Ellis, *ACS Catal.*, 2018, **8**, 5732–5776; (*c*) Z. Wang, J. Ni, Y. Kuninobu and M. Kanai, *Angew. Chem., Int. Ed.*, 2014, **53**, 3496–3499; (*d*) G. He, S. Zhang, W. Nack, Q. Li and G. Chen, *Angew. Chem., Int. Ed.*, 2013, **52**, 11124–11128; (*e*) X. Wu, Y. Zhao and H. Ge, *Chem.–Eur. J.*, 2014, **20**, 9530–9533; (*f*) J. J. Neumann, S. Rakshi, T. Dröge and F. Glorius, *Angew. Chem., Int. Ed.*, 2009, **48**, 6892–6895.

12 J. A. Labinger and J. E. Bercaw, *Nature*, 2002, **417**, 507–514.

13 (*a*) Y. Tan and J. F. Hartwig, *J. Am. Chem. Soc.*, 2010, **132**, 3676–3677; (*b*) S. W. Youn, J. H. Bihn and B. S. Kim, *Org. Lett.*, 2011, **13**, 3738–3741; (*c*) J. F. Hartwig, *Inorg. Chem.*, 2007, **46**, 1936–1947; (*d*) J. A. Jordan-Hore, C. C. C. Johansson, M. Gulias, E. M. Beck and M. J. Gaunt, *J. Am. Chem. Soc.*, 2008, **130**, 16184–16186.

14 A. Studer, *Chem.–Eur. J.*, 2001, **7**, 1159–1164.

15 (*a*) S. P. West, A. Bisai, A. D. Lim, R. R. Narayan and R. Sarpong, *J. Am. Chem. Soc.*, 2009, **131**, 11187–11194; (*b*) J. M. Gruver, S. P. West, D. B. Collum and R. Sarpong, *J. Am. Chem. Soc.*, 2010, **132**, 13212–13213; (*c*) J. L. Jeffrey, E. B. Bartlett and R. Sarpong, *Angew. Chem., Int. Ed.*, 2013, **52**, 2194–2197.

16 (*a*) M. A. Syroeshkin, F. Kuriakose, E. A. Saverina, V. A. Timofeeva, M. P. Egorov and I. V. Alabugin, *Angew. Chem., Int. Ed.*, 2019, **58**, 5532–5550; (*b*) A. Studer and D. P. Curran, *Nat. Chem.*, 2014, **6**, 765–773.

17 For the general review of dehydrogenative C–O bond formation, see: I. B. Krylov, V. A. Vil' and A. O. Terent'ev, Cross-dehydrogenative Coupling for the Intermolecular C-O Bond Formation, *Beilstein J. Org. Chem.*, 2015, **11**, 92–146.

18 D.-M. Yan, Q.-Q. Zhao, L. Rao, J.-R. Chen and W.-J. Xiao, *Chem.–Eur. J.*, 2018, **24**, 16895–16901.

19 U. S. Department of Health and Human Services Food and Drug Administration, *Q3D Elemental Impurities Guidance for Industry*, 2015.

20 J. G. Topliss, L. M. Konzelman, N. Sperber and E. R. Franklin, *J. Med. Chem.*, 1964, **7**, 453–456.

21 (*a*) I. R. Hardcastle, S. U. Ahmed, H. Atkins, G. Farnie, B. T. Golding, R. J. Griffin, S. Guyenne, C. Hutton, P. Källblad, S. J. Kemp, M. S. Kitching, D. R. Newell, S. Norbedo, J. Northen, R. J. Reid, K. Saravanan, H. M. Willems and J. Lunec, *J. Med. Chem.*, 2006, **49**, 6209–6221; (*b*) C. Riedinger, J. A. Endicott, S. J. Kemp, L. A. Smyth, A. Watson, E. Valeur, B. T. Golding, R. J. Griffin, I. R. Hardcastle, M. E. Noble and J. M. McDonnell, *J. Am. Chem. Soc.*, 2008, **130**, 16038–16044; (*c*) I. R. Hardcastle, J. Liu, E. Valeur, A. Watson, S. U. Ahmed, T. J. Blackburn, K. Bennaceur, W. Clegg, C. Drummond, J. A. Endicott, B. T. Golding, R. J. Griffin, J. Gruber, K. Haggerty, R. W. Harrington, C. Hutton, S. Kemp, X. Lu, J. M. McDonnell, D. R. Newell, M. E. Noble, S. L. Payne, C. H. Revill, C. Riedinger, Q. Xu and J. Lunec, *J. Med. Chem.*, 2011, **54**, 1233–1243; (*d*) A. F. Watson, J. Liu, K. Bennaceur, C. J. Drummond, J. A. Endicott, B. T. Golding, R. J. Griffin, K. Haggerty, X. Lu, J. M. McDonnell, D. R. Newell, M. E. M. Noble, C. H. Revill, C. Riedinger, Q. Xu, Y. Zhao, J. Lunec and I. R. Hardcastle, *Bioorg. Med. Chem. Lett.*, 2011, **21**, 5916–

5919; (*e*) T. A. Grigoreva, D. S. Novikova, A. V. Petukhov, M. A. Gureev, A. V. Garabadzhiu, G. Melino, N. A. Barlevv and V. G. Tribulovich, *Bioorg. Med. Chem. Lett.*, 2017, **27**, 5197–5202.

22 (*a*) V. Fajardo, V. Elango, B. K. Cassels and M. Shamma, *Tetrahedron Lett.*, 1982, **23**, 39–42; (*b*) H. Kamauchi, Y. Shiraishi, A. Kojima, N. Kawazoe, L. Kinoshita and K. Koyama, *J. Nat. Prod.*, 2018, **81**, 1290–1294.

23 M.-W. Chen, Q.-A. Chen, Y. Duan, Z.-S. Ye and Y.-G. Zhou, *Chem. Commun.*, 2012, **48**, 1698–1700.

24 Z. Kang, D. Zhang, J. Shou and W. Hu, *Org. Lett.*, 2018, **20**, 983–986.

25 (*a*) T. Nishimura, M. Nagamoto, Y. Ebe and T. Hayashi, *Chem. Sci.*, 2013, **4**, 4499–4504; (*b*) S. Sharma, Y. Oh, N. K. Mishra, U. De, H. Jo, R. Sachan, H. S. Kim, Y. H. Jung and I. S. Kim, *J. Org. Chem.*, 2017, **82**, 3359–3367; (*c*) M. Nagamoto and T. Nishimura, *Chem. Commun.*, 2014, **50**, 6274–6277; (*d*) T. Nishimura, A. Noishiki, Y. Ebe and T. Hayashi, *Angew. Chem., Int. Ed.*, 2013, **52**, 1777–1780.

26 (*a*) H. H. Wasserman and J. l. Ives, *Tetrahedron*, 1981, **37**, 1825–1852; (*b*) P. R. Ogilby, *Chem. Soc. Rev.*, 2010, **39**, 3181–3209; (*c*) A. A. Ghogare and A. Greer, *Chem. Rev.*, 2016, **116**, 9994–10034.

27 (*a*) Y. Gao, G. Hu, J. Zhong, Z. Shi, Y. Zhu, D. Su and J. Wang, *Angew. Chem., Int. Ed.*, 2013, **52**, 2109–2113; (*b*) G. Urgoita, R. SanMartin, M. T. Herrero and E. Domínguez, *Chem. Commun.*, 2015, **51**, 4799–4802; (*c*) J. Ma, Z. Hu, M. Li, W. Zhao, X. Hu, W. Mo, B. Hu, N. Sun and Z. Shen, *Tetrahedron*, 2015, **71**, 6733–6739; (*d*) H. Wang, Z. Wang, H. Huang, J. Tan and K. Xu, *Org. Lett.*, 2016, **18**, 5680–5683; (*e*) C. Guo, Y. Zhang, Y. Zhang and J. Wang, *Chem. Commun.*, 2018, **54**, 3701–3704; (*f*) H. Sterckx, B. Morel and B. U. W. Maes, *Angew. Chem., Int. Ed.*, 2019, **58**, 7946–7970.

28 The M06-2X functional has demonstrated to provide good thermodynamic data for organic reactions. For more details, see: (*a*) Y. Zhao and D. G. Truhlar, *Theor. Chem. Acc.*, 2008, **120**, 215–241; (*b*) Y. Zhao and D. G. Truhlar, *Acc. Chem. Res.*, 2008, **41**, 157–167.

29 A. V. Marenich, C. J. Cramer and D. G. Truhlar, *J. Phys. Chem. B*, 2009, **113**, 6378.

30 S. Grimme, J. Antony, S. Ehrlich and H. Krieg, *J. Chem. Phys.*, 2010, **132**, 154104.

31 M. J. Frisch, G. W. Trucks, H. B. Schlegel, G. E. Scuseria, M. A. Robb, J. R. Cheeseman, G. Scalmani, V. Barone, B. Mennucci, G. A. Petersson, H. Nakatsuji, M. Caricato, X. Li, H. P. Hratchian, A. F. Izmaylov, J. Bloino, G. Zheng, J. L. Sonnenberg, M. Hada, M. Ehara, K. Toyota, R. Fukuda, J. Hasegawa, M. Ishida, T. Nakajima, Y. Honda, O. Kitao, H. Nakai, T. Vreven, J. A. Montgomery Jr, J. E. Peralta, F. Ogliaro, M. Bearpark, J. J. Heyd, E. Brothers, K. N. Kudin, V. N. Staroverov, R. Kobayashi, J. Normand, K. Raghavachari, A. Rendell, J. C. Burant, S. S. Iyengar, J. Tomasi, M. Cossi, N. Rega, M. J. Millam, M. Klene, J. E. Knox, J. B. Cross, V. Bakken, C. Adamo, J. Jaramillo, R. Gomperts, R. E. Stratmann, O. Yazyev, A. J. Austin, R. Cammi, C. Pomelli, J. W. Ochterski, R. L. Martin, K. Morokuma, V. G. Zakrzewski, G. A. Voth, P. Salvador, J. J. Dannenberg, S. Dapprich, A. D. Daniels, Ö. Farkas, J. B. Foresman, J. V. Ortiz, J. Cioslowski and D. J. Fox, Gaussian, Inc., Wallingford CT, 2009.

32 C. Y. Legault, *CYLview, 1.0b*, Université de Sherbrooke, 2009, http://www.cylview.org.

33 *ChemCraft 1.8*, http://www.chemcraftprog.com, accessed in February 2016.

34 (*a*) Y.-Y. Chen, X.-J. Zhang, H.-M. Yuan, W.-T. Wei and M. Yan, *Chem. Commun.*, 2013, **49**, 10974–10976; (*b*) W.-J. Wang, X. Zhao, L. Tong, J.-H. Chen, X.-J. Zhang and M. Yan, *J. Org. Chem.*, 2014, **79**, 8557–8565; (*c*) Y.-Y. Chen, N.-N. Zhang, L.-M. Ye, J.-H. Chen, X. Sun, X.-J. Zhang and M. Yan, *RSC Adv.*, 2015, **5**, 48046–48049; (*d*) W.-T. Wei, Y.-J. Cheng, Y. Hu, Y.-Y. Chen, X.-J. Zhang, Y. Zou and M. Yan, *Adv. Synth. Catal.*, 2015, **357**, 3474–3478; (*e*) Y.-Y. Chen, Z.-Y. Chen, N.-N. Zhang, J.-H. Chen, X.-J. Zhang and M. Yan, *Eur. J. Org. Chem.*, 2016, **3**, 599–606.

35 E. J. Nanni Jr, M. D. Stallings and D. T. Sawyer, *J. Am. Chem. Soc.*, 1980, **102**, 4481–4485.

36 M. Pichette Drapeau, I. Fabre, L. Grimaud, I. Ciofini, T. Ollevier and M. Taillefer, *Angew. Chem., Int. Ed.*, 2015, **54**, 10587–10591.

37 J.-S. Li, F. Yang, Q. Yang, Z.-L. Li, G.-Q. Chen, Y.-D. Da, P.-M. Huang, C. Chen, Y. Zhang and L.-Z. Huang, *Synlett*, 2017, **28**, 994–998.

38 For the effect of such geometric changes on stability and reactivity, see: I. V. Komarov, S. Yanik, A. Y. Ishchenko, J. E. Davies, J. M. Goodman and A. J. Kirby, *J. Am. Chem. Soc.*, 2015, **137**, 926–930; M. Hutchby, C. E. Houlden, M. F. Haddow, S. N. G. Tyler, G. C. Lloyd-Jones and K. I. Booker-Milburn, *Angew. Chem.*, 2012, **124**, 563–566; M. Szostak and J. Aube, *Chem. Rev.*, 2013, **113**, 5701–5765; S. Z. Vatsadze, Y. D. Loginova, G. Gomes and I. V. Alabugin, *Chem.–Eur. J.*, 2017, **23**, 3225–3245.

39 P. Peterson, N. Shevchenko, B. Breiner, M. Manoharan, F. Lufti, J. Delaune, M. Kingsley, K. Kovnir and I. V. Alabugin, *J. Am. Chem. Soc.*, 2016, **138**, 15617–15628.

40 F. A. Cotton, G. Wilkinson, C. A. Murillo and M. Bochmann, *Advanced Inorganic Chemistry*, Wiley, New York, 6th edn, 1999, p. 461.

41 G. W. Burton and K. U. Ingold, *J. Am. Chem. Soc.*, 1981, **103**, 6472–6477.

42 (*a*) E. Bothe, M. N. Schuchmann, D. Schulte-Frohlinde and C. Sonntag, *Z. Naturforsch., B: J. Chem. Sci.*, 1983, **38**, 212–219; (*b*) W. Song, T. Xu, W. J. Cooper, D. D. Dionysiou, A. A. d. l. Cruz and K. E. O'Shea, *Environ. Sci. Technol.*, 2009, **43**, 1487–1492; (*c*) L. M. Dorfman and G. E. Adams, *Reactivity of the Hydroxyl Radical in Aqueous Solutions*, U.S. National Bureau of Standards, Washington, DC, 1973; (*d*) H. Chen, L. Lin, Z. Lin, G. Guo and J. M. Lin, *J. Phys. Chem. A*, 2010, **114**, 10049–10058.

43 (*a*) E. J. Nanni, D. T. Sawyer, S. S. Ball and T. C. Bruice, *J. Am. Chem. Soc.*, 1981, **103**, 2797–2802; (*b*) D. T. Sawyer, E. J. Nanni and J. L. Roberts Jr, *Electrochemical and Spectrochemicla Studies of Biological Redox Components*, 1982, pp. 585–600; (*c*) M. Hayyan, M. A. Hasim and I. M. AlNashef, *Chem. Rev.*, 2016, **116**, 3029–3085.

44 (*a*) E. J. Nanni Jr, M. D. Stallings and D. T. Sawyer, *J. Am. Chem. Soc.*, 1980, **102**, 4481–4485; (*b*) D.-H. Chin, G. Chiericato Jr, E. J. Nanni Jr and D. T. Sawyer, *J. Am. Chem. Soc.*, 1982, **104**, 1296–1299.

45 Note that the peroxide moiety in this molecule would engage in the anomeric $nO \rightarrow \sigma^{*}_{C-N}$ interaction. Such interactions were shown to significantly stabilize peroxides with geminal acceptor groups: (*a*) G. P. Gomes, V. Vil', A. Terent'ev and I. V. Alabugin, *Chem. Sci.*, 2015, **6**, 6783–6791; (*b*) V. A. Vil', G. P. Gomes, M. V. Ekimova, K. A. Lyssenko, M. A. Syroeshkin, G. I. Nikishin, I. V. Alabugin and A. O. Terent'ev, *J. Org. Chem.*, 2018, **83**, 13427–13445; (*c*) E. Juaristi, G. P. Gomes, A. O. Terent'ev, R. Notario and I. V. Alabugin, *J. Am. Chem. Soc.*, 2017, **139**, 10799–10813; (*d*) G. P. Gomes, I. A. Yaremenko, P. S. Radulov, R. A. Novikov, V. V. Chernyshev, A. A. Korlyukov, G. I. Nikishin, I. V. Alabugin and A. O. Terent'ev, *Angew. Chem., Int. Ed.*, 2017, **56**, 4955–4959.

46 D. Swern, A. H. Clements and T. M. Lung, *Anal. Chem.*, 1969, **41**, 412–416.

47 (*a*) D. M. Schultz, F. Levesque, D. A. DiRocco, M. Reibarkh, Y. Ji, L. A. Joyce, J. F. Dropinski, H. Sheng, B. D. Sherry and I. W. Davies, *Angew. Chem., Int. Ed.*, 2017, **56**, 15274–15278; (*b*) A. S.-K. Tsang, A. Kapat and F. Schoenebeck, *J. Am. Chem. Soc.*, 2016, **138**, 518–526; (*c*) K.-J. Liu, Z.-H. Duan, X.-L. Zeng, M. Sun, Z. Tang, S. Jiang, Z. Cao and W.-M. He, *ACS Sustainable Chem. Eng.*, 2019, **7**, 10293–10298; (*d*) M. Lesieur, C. Genicot and P. Pasau, *Org. Lett.*, 2018, **20**, 1987–1990.

48 (*a*) M. Griesser, R. Shah, A. T. Van Kessel, O. Zilka, E. A. Haidasz and D. A. Pratt, *J. Am. Chem. Soc.*, 2018, **140**, 3798–3808; (*b*) A. Samuni, C. M. Krishna, P. Riesz, E. Finkelstein and A. Russo, *J. Biol. Chem.*, 1988, **263**, 17921–17924; (*c*) J. B. Mitchell, A. Samuni, M. C. Krishna, W. G. DeGraff, M. S. Ahn, U. Samuni and A. Russo, *Biochemistry*, 1990, **29**, 2802–2807; (*d*) M. C. Krishna, D. A. Grahame, A. Samuni, J. B. Mitchell and A. Russo, *Proc. Natl. Acad. Sci. U. S. A.*, 1992, **89**, 5537–5541; (*e*) M. C. Krishna, A. Russo, J. B. Mitchell, S. Goldstein, H. Dafni and A. Samuni, *J. Biol. Chem.*, 1996, **271**, 26026–26031.

49 (*a*) J. M. Bobbit, C. Brückner and N. Merbouh, *Org. React.*, 2009, **74**, 103; (*b*) H. Richter and O. G. Mancheño, *Eur. J. Org. Chem.*, 2010, **2010**, 4460–4467; (*c*) A. J. Neel, J. P. Hehn, P. F. Tripet and F. D. Toste, *J. Am. Chem. Soc.*, 2013, **135**, 14044–14047; (*d*) K. T. Tarantino, D. C. Miller, T. A. Callon and R. R. Knowles, *J. Am. Chem. Soc.*, 2015, **137**, 6440–6443.

50 Z. Zhang, Y. Gao, Y. Liu, J. Li, H. Xie, H. Li and W. Wang, *Org. Lett.*, 2015, **17**, 5492–5495.

51 (*a*) M. F. Semmelhack, C. R. Schmid and D. A. Cortes, *Tetrahedron Lett.*, 1986, **27**, 1119–1122; (*b*) T. A. Hamlin, C. B. Kelly, J. M. Ovian, R. J. Wiles, L. J. Tilley and N. E. Leadbeater, *J. Org. Chem.*, 2015, **80**, 8150–8167; (*c*) H. Richter and O. G. Mancheño, *Eur. J. Org Chem.*, 2010, 4460–4467; (*d*) J. Dong, Q. Xia, C. Yan, H. Song, Y. Liu and Q. Wang, *J. Org. Chem.*, 2018, **83**, 4516–4524.